Ultra-Peripheral Physics with ATLAS

Ben Gilbert, on behalf of the ATLAS Collaboration
PANIC 2021

UPC and Non-UPC Events

- The intense electromagnetic fields surrounding the nuclei in heavy ion collisions provide a flux of quasi-real photons for both $\gamma\gamma$ and γA processes.
  - ATLAS has developed a robust physics program studying both of these collision systems.
- Ultra-Peripheral Collisions (UPC) -- Photon-initiated collisions with no hadronic contribution
- Non-UPC -- Collisions with a hadronic contribution and photon-initiated processes in the background

UPC Event

$b_{imp} > R_1 + R_2$

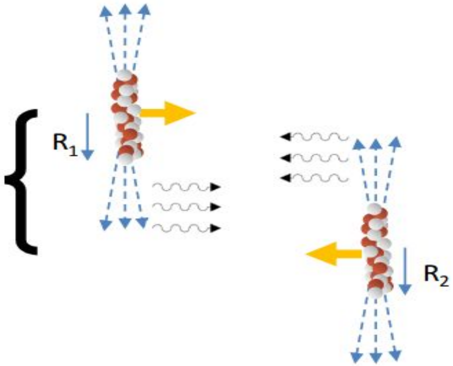

Non-UPC Event

$b_{imp} < R_1 + R_2$

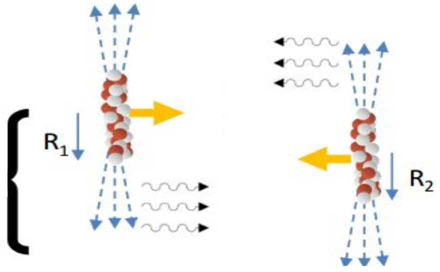

Why Study Ultra-Peripheral Collisions?

- What has ATLAS measured recently using photon-induced processes?
  - UPC Dimuons: A standard candle for photoproduction in Heavy Ion collisions
  - Non-UPC Dimuons: Using $\gamma\gamma \rightarrow \mu^{+}\mu^{-}$ as an electromagnetic probe of Quark-Gluon Plasma
  - Light-by-light scattering: Fundamental QED and setting bounds on BSM physics using UPC
  - Photonuclear Flow: Investigating system-size limits on QCD systems exhibiting collectivity

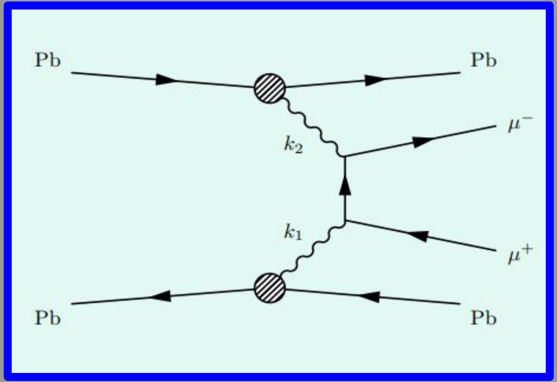

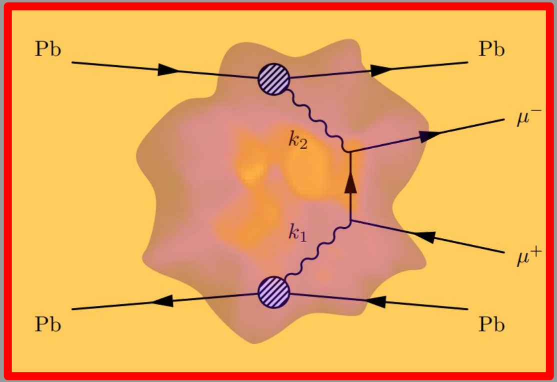

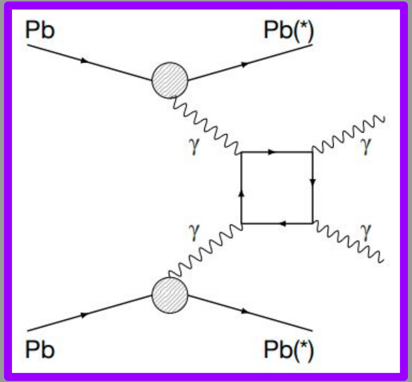

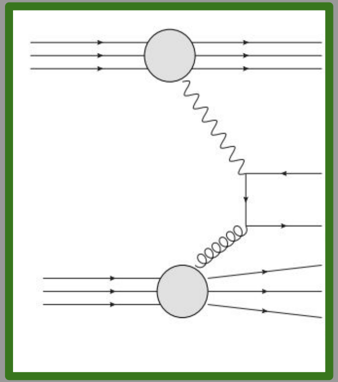

Dimuon Production in Ultra-Peripheral Collisions

- The ATLAS UPC dimuon measurement includes 3 $\gamma\gamma \rightarrow \mu^+\mu^-$ processes.

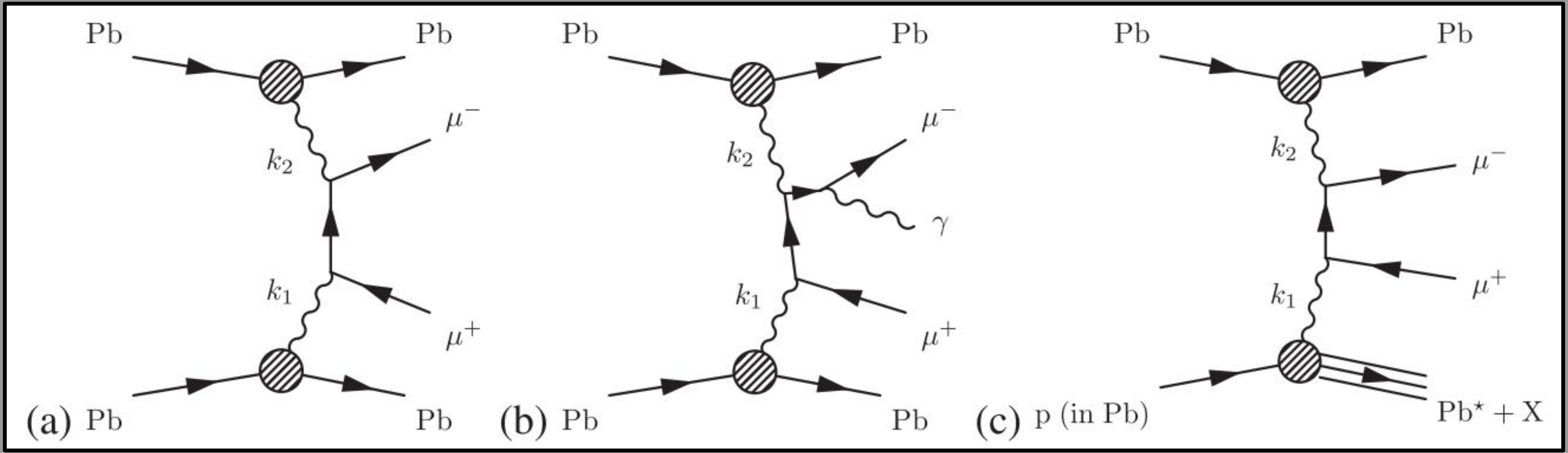

Dimuon Production in Ultra-Peripheral Collisions

- The ATLAS UPC dimuon measurement includes 3 $\gamma\gamma\rightarrow\mu^{+}\mu^{-}$ processes.
  - Left: Leading-order QED Process (Breit-Wheeler)

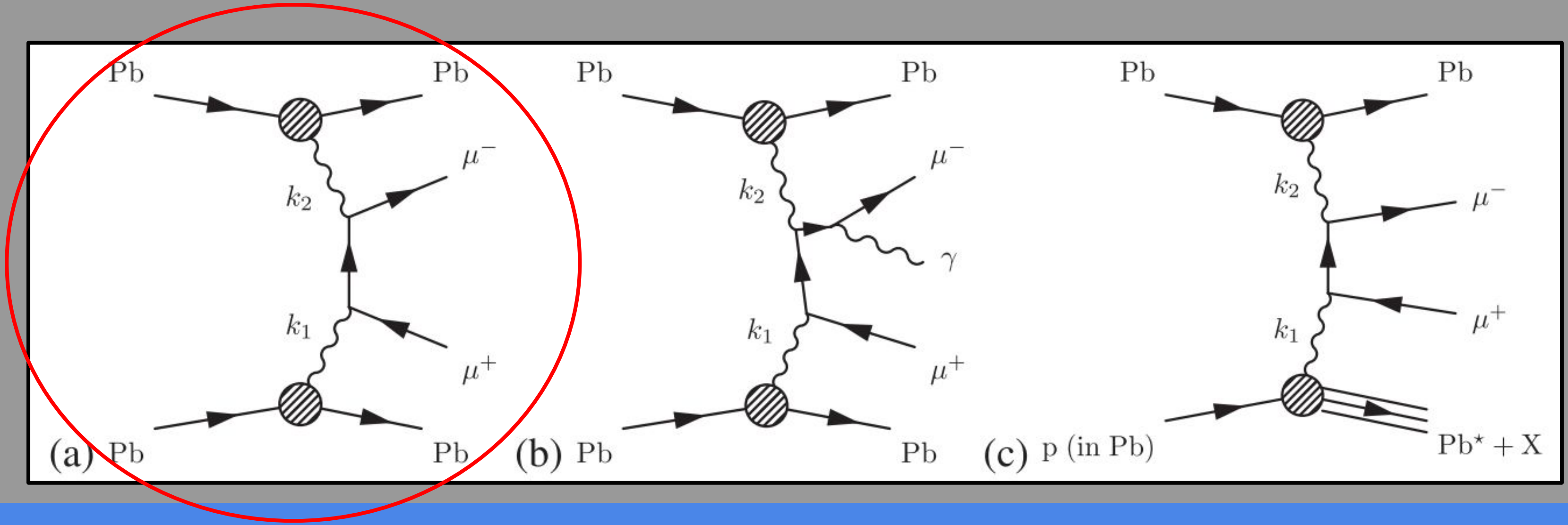

Dimuon Production in Ultra-Peripheral Collisions

- The ATLAS UPC dimuon measurement includes 3 $\gamma\gamma\rightarrow\mu^+\mu^-$ processes.
  - Left: Leading-order QED Process (Breit-Wheeler)
  - Middle: Final-state QED Showering (Radiative)

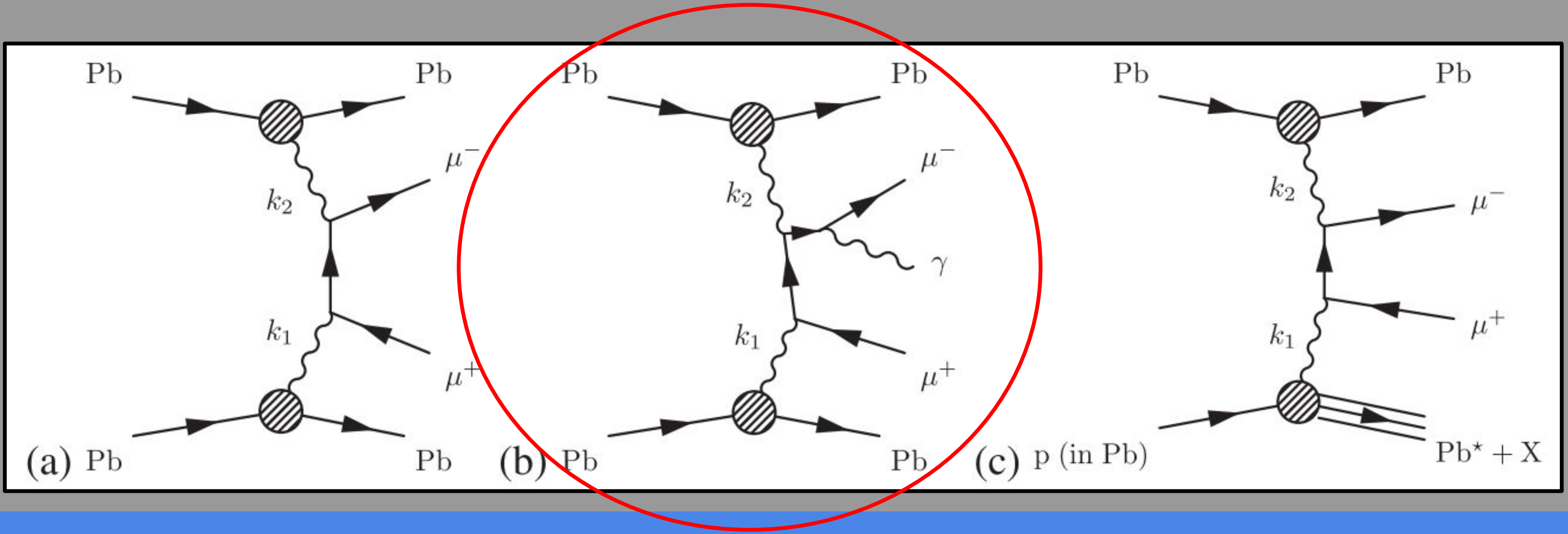

Dimuon Production in Ultra-Peripheral Collisions

- The ATLAS UPC dimuon measurement includes 3 $\gamma\gamma \rightarrow \mu^+\mu^-$ processes.
  - Left: Leading-order QED Process (Breit-Wheeler)
  - Middle: Final-state QED Showering (Radiative)
  - Right: Nuclear break-up modifies the initial photon energy (Dissociative)

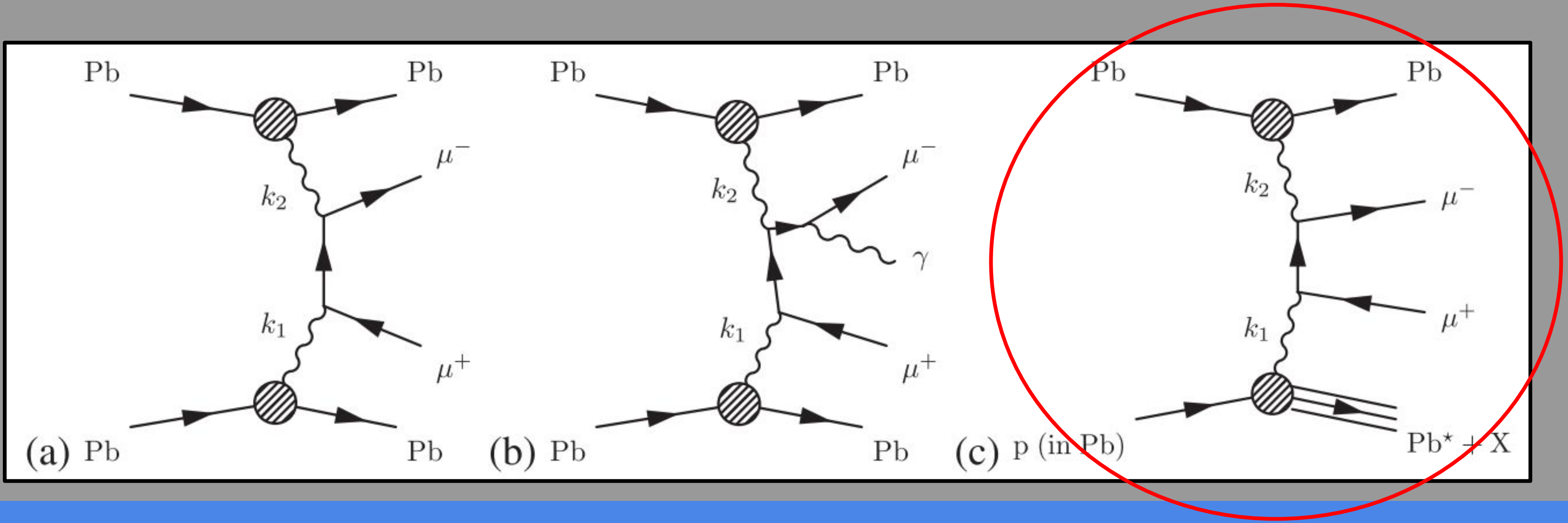

Dimuon Production in Ultra-Peripheral Collisions

- The ATLAS UPC dimuon measurement includes 3 $\gamma\gamma\rightarrow\mu^{+}\mu^{-}$ processes.
  - Left: Leading-order QED Process (Breit-Wheeler)
  - Middle: Final-state QED Showering (Radiative)
  - Right: Nuclear break-up modifies the initial photon energy (Dissociative)
- The Zero-Degree Calorimeter (ZDC) helps separate these different contributions.

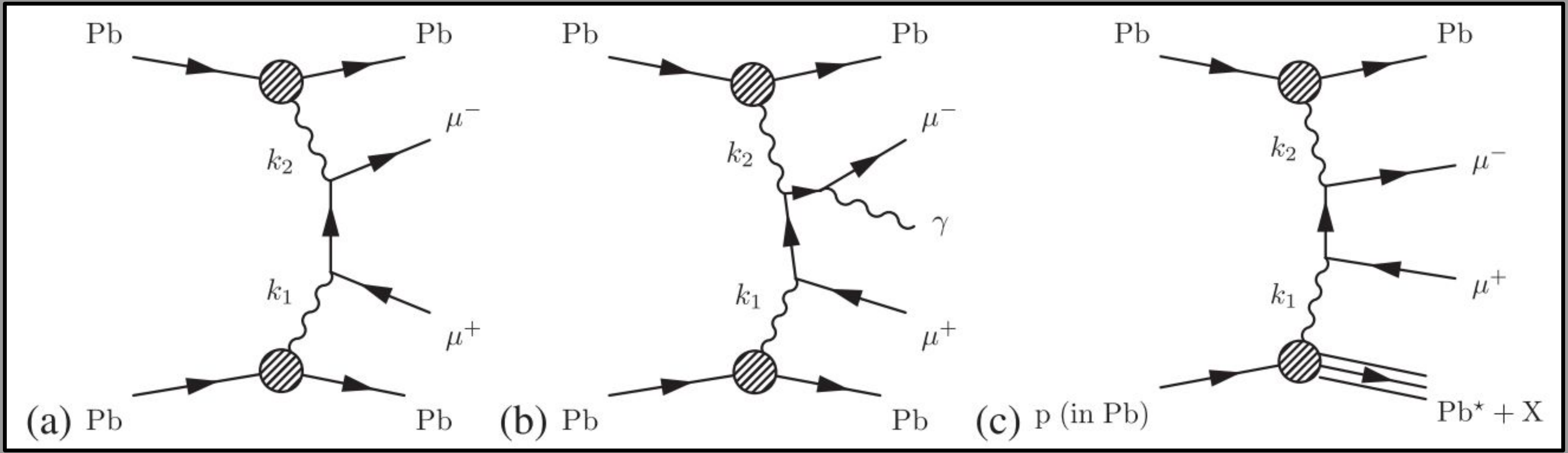

ZDC Topology in UPC Dimuon Production

- Here, the 2D ZDC energy distribution of events passing other fiducial selections shows 3 clear event classes.

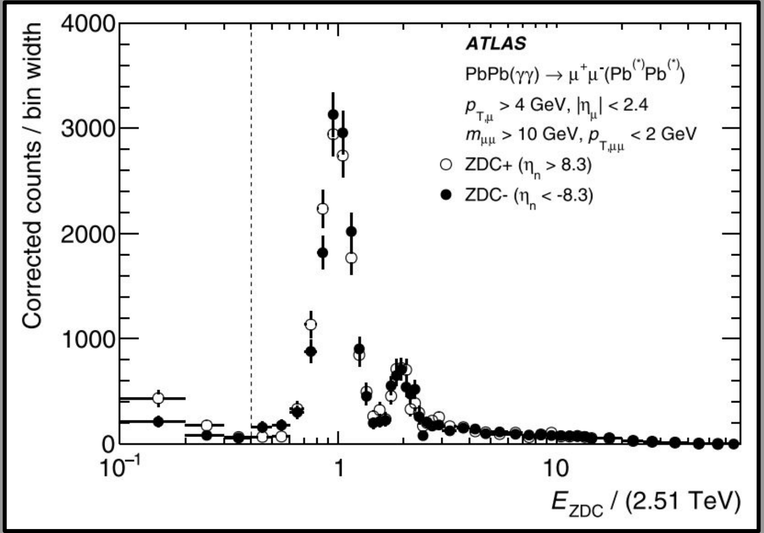

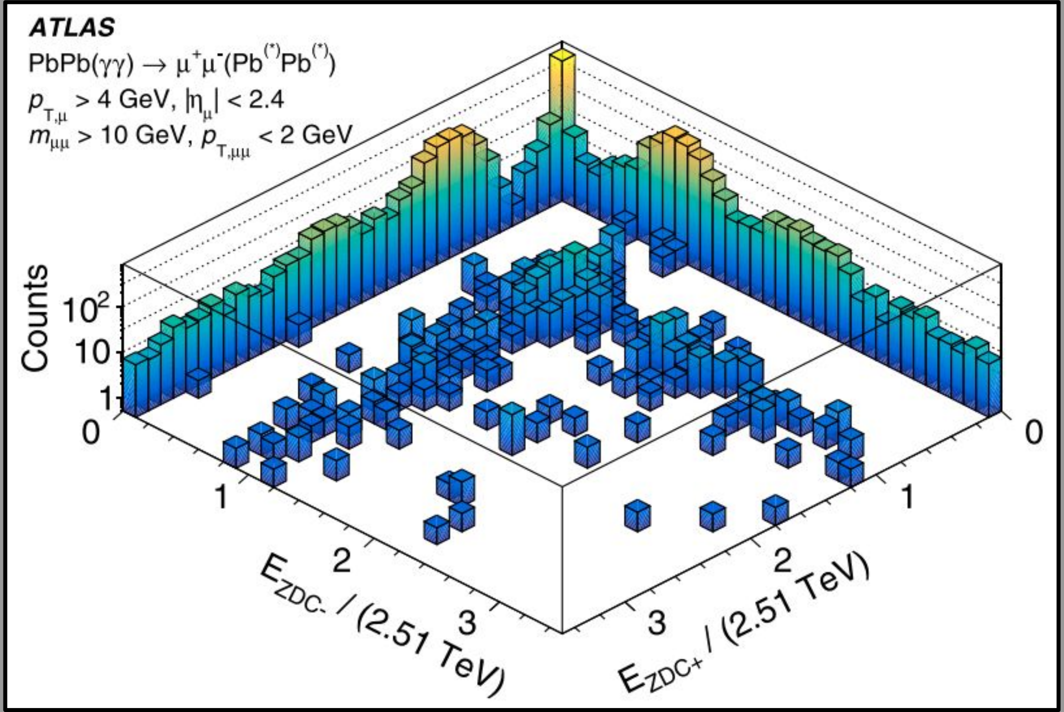

ZDC Topology in UPC Dimuon Production

- Here, the 2D ZDC energy distribution of events passing other fiducial selections shows 3 clear event classes.

0n0n: No neutrons emitted on either side of the detector (No nuclear break-up)

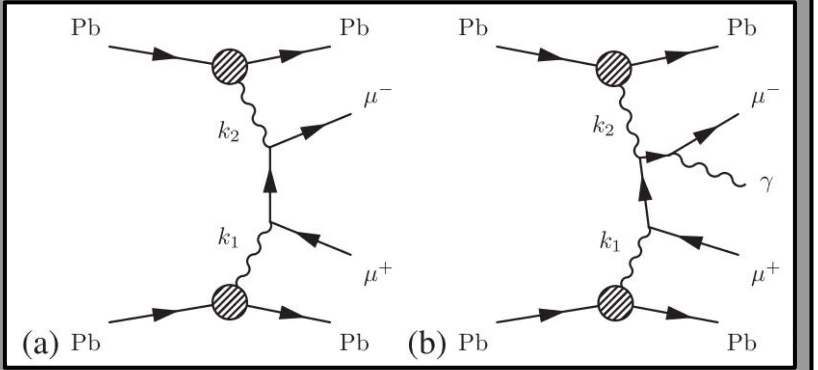

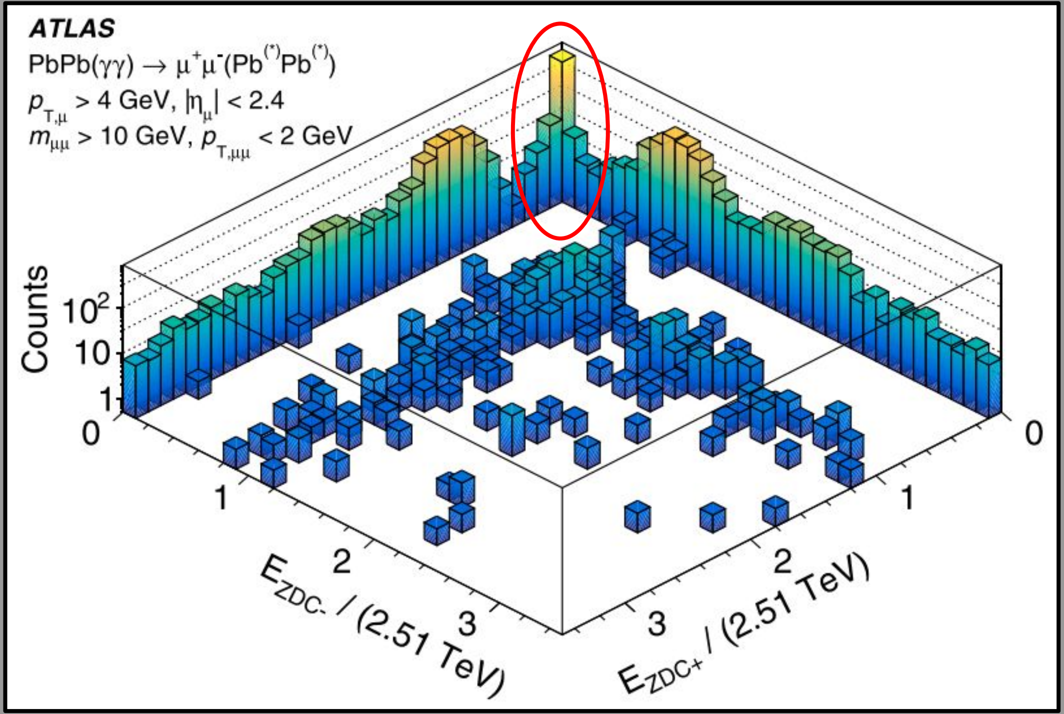

ZDC Topology in UPC Dimuon Production

- Here, the 2D ZDC energy distribution of events passing other fiducial selections shows 3 clear event classes.

0nXn: Neutrons emitted on one side of the detector (Single-dissociative)

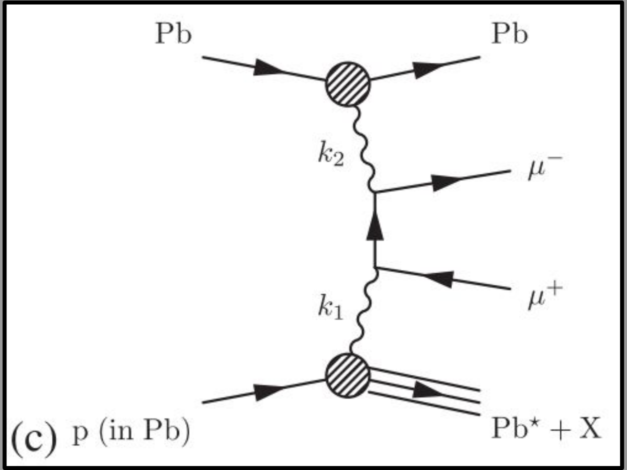

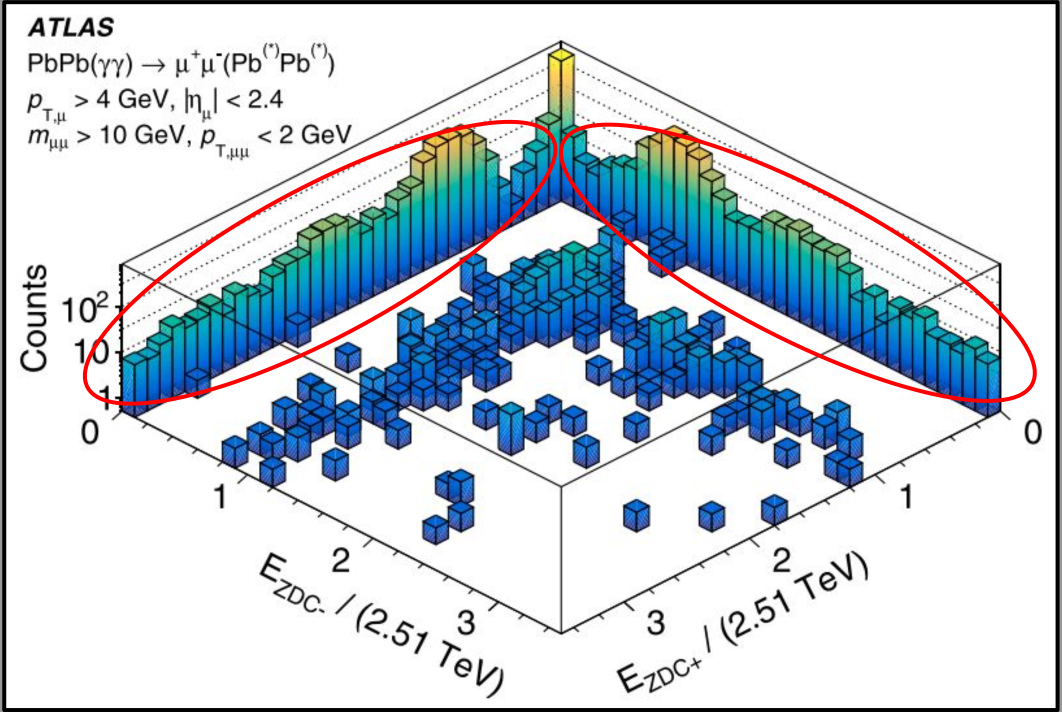

ZDC Topology in UPC Dimuon Production

- Here, the 2D ZDC energy distribution of events passing other fiducial selections shows 3 clear event classes.

XnXn: Neutrons emitted on both sides of the detector (Double-dissociative)

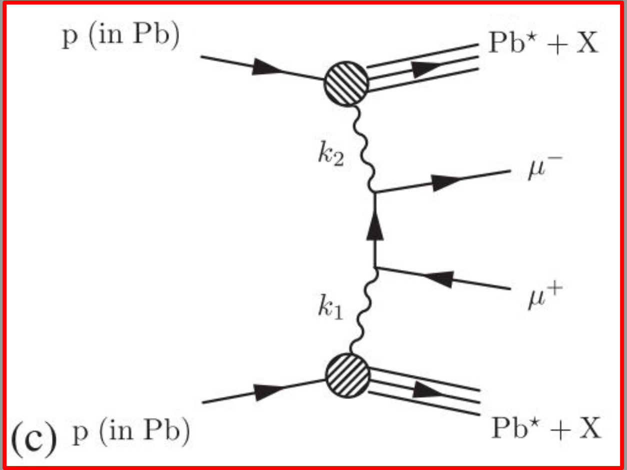

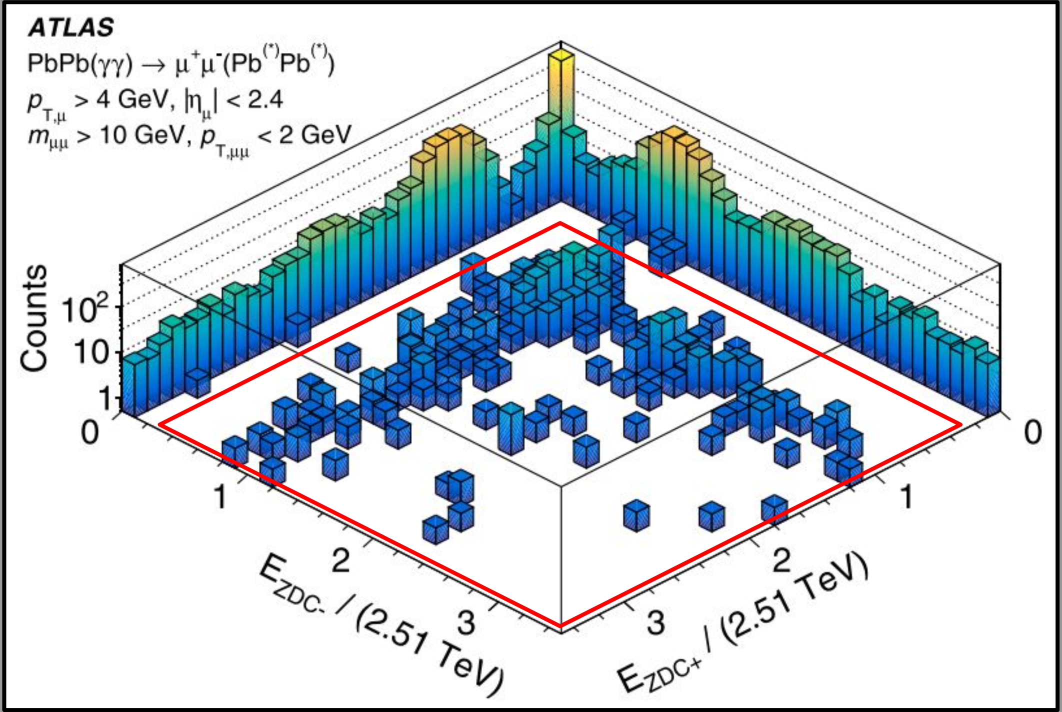

Acoplanarity Distributions

- These different acoplanarity distributions arise from cutting on ZDC topologies.

$$\alpha \equiv 1 - |\Delta\phi|/\pi$$

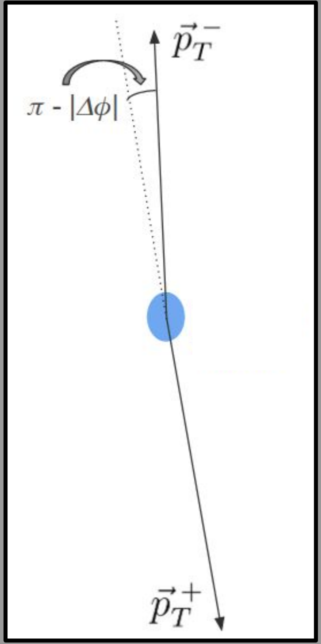

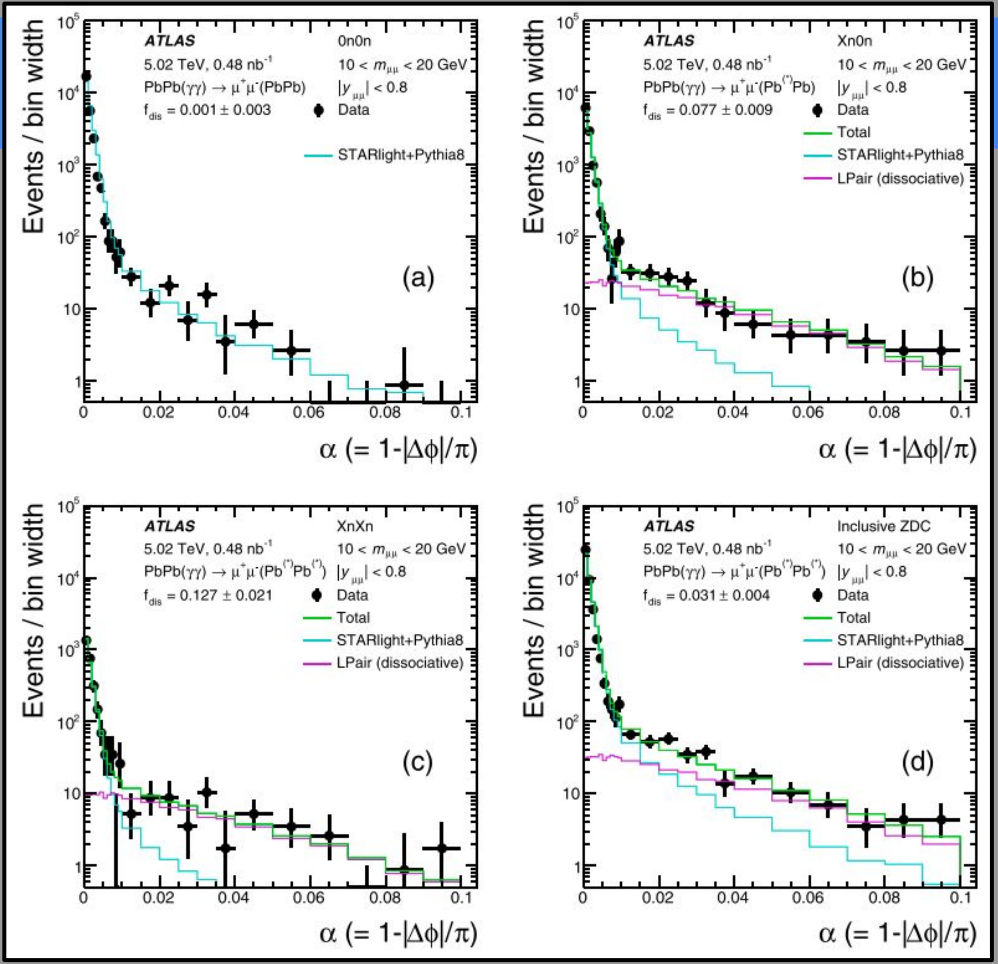

Acoplanarity Distributions

- These different acoplanarity distributions arise from cutting on ZDC topologies.
- Template fits of the different contributions help to experimentally determine f_{dis}, the dissociative fraction.
  - The QED contribution comes from STARlight+Pythia8.
  - The dissociative contribution comes from LPair.

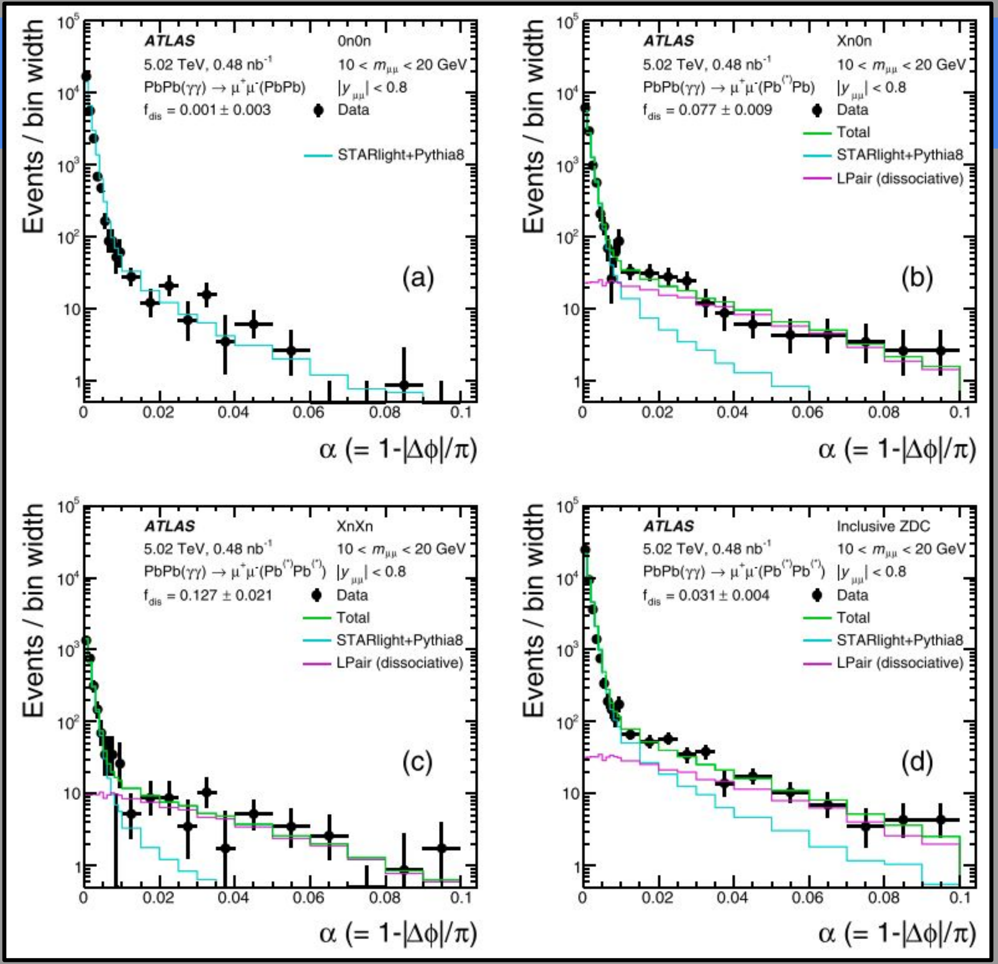

Acoplanarity Distributions

- These different acoplanarity distributions arise from cutting on ZDC topologies.
- Template fits of the different contributions help to experimentally determine f_{dis}, the dissociative fraction.
  - The QED contribution comes from STARlight+Pythia8.
  - The dissociative contribution comes from LPair.
- The dissociative part dominates in the tails for 0nXn and XnXn.
  - ZDC topology cuts can effectively filter out the dissociative contribution.

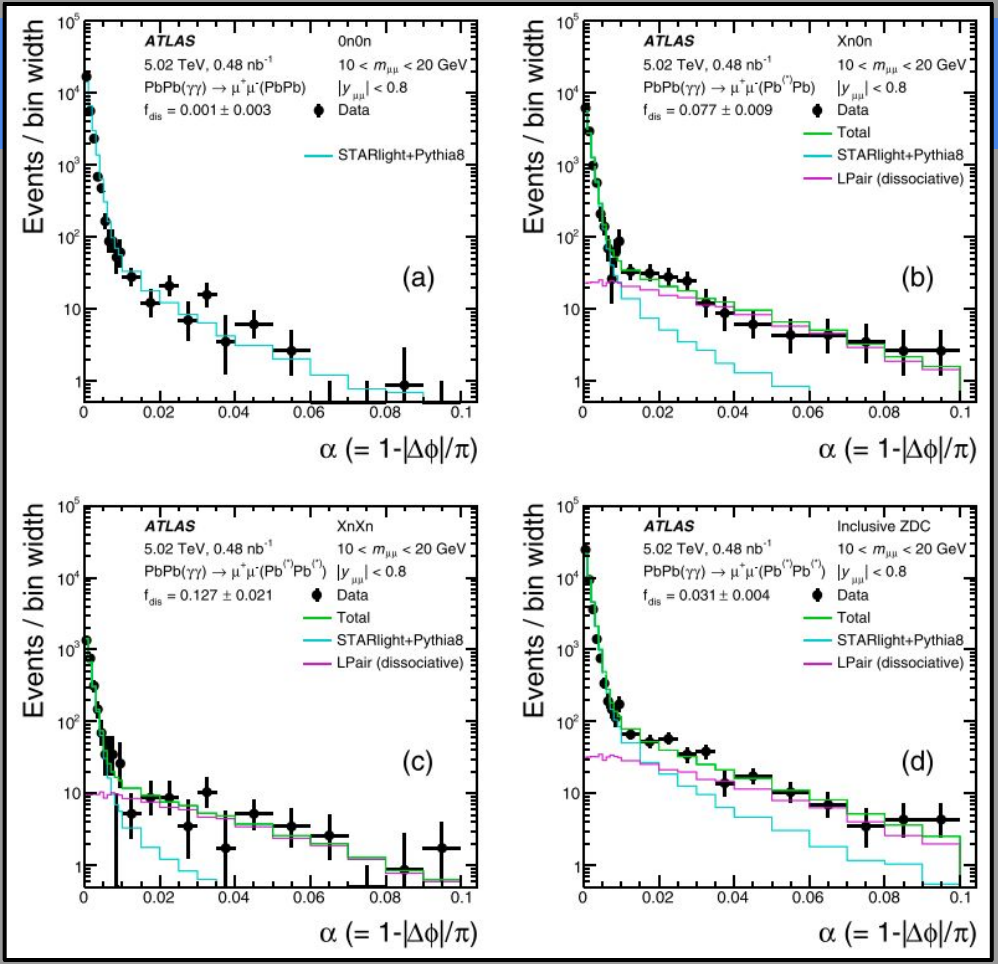

Measuring the Photon Flux

- The colliding photon energies can be determined from the dimuon pair kinematics:

$$k_{max,min} = \frac{m_{\mu\mu}}{2} e^{\pm y_{\mu\mu}}$$

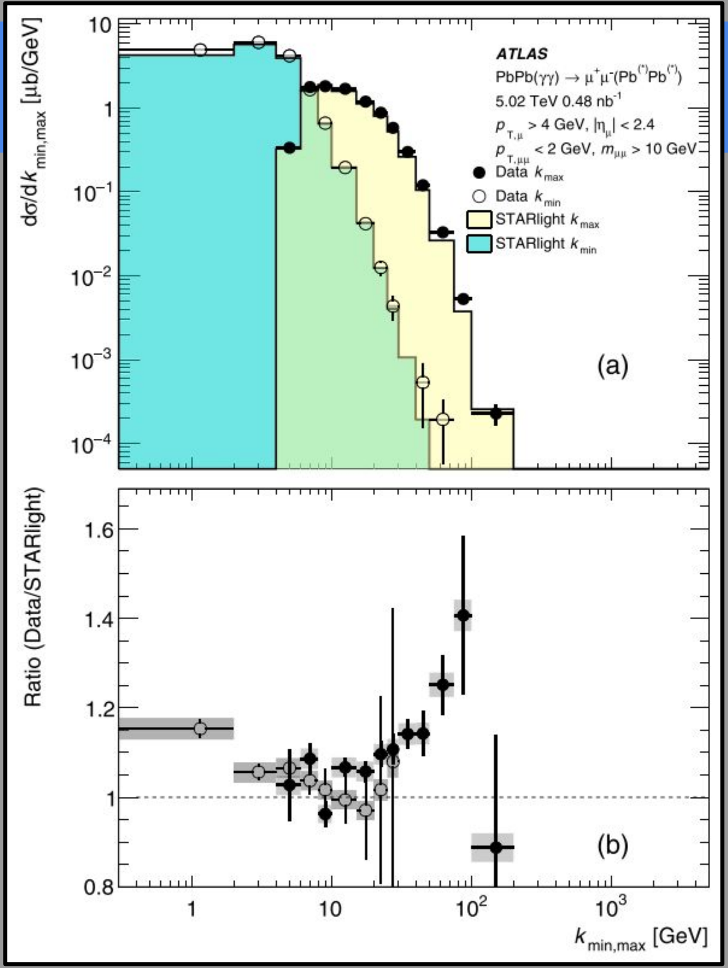

Measuring the Photon Flux

- The colliding photon energies can be determined from the dimuon pair kinematics:

$$k_{max,min} = \frac{m_{\mu\mu}}{2} e^{\pm y_{\mu\mu}}$$

- This result is the first direct measurement of the nuclear photon flux.
  - Some differences arise from the non-zero dissociative fraction, as shown on previous slides.

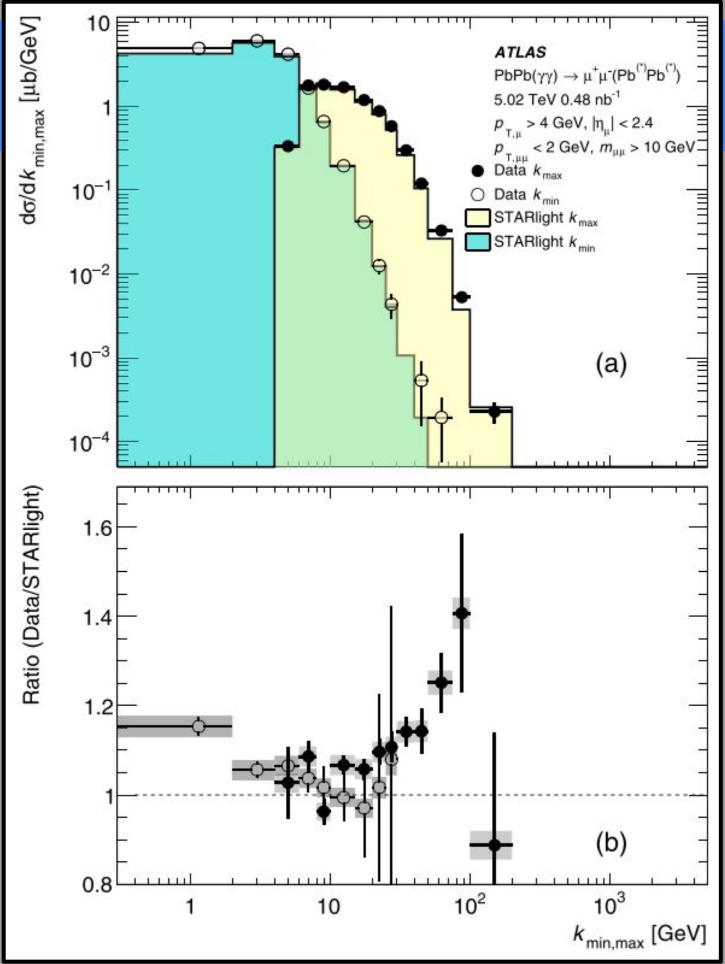

Measuring the Photon Flux

- The colliding photon energies can be determined from the dimuon pair kinematics:

$$k_{max,min} = \frac{m_{\mu\mu}}{2} e^{\pm y_{\mu\mu}}$$

- This result is the first direct measurement of the nuclear photon flux.
  - Some differences arise from the non-zero dissociative fraction, as shown on previous slides.
- The agreement with STARlight is already quite good, with some key differences.
  - The data k_{max} distribution has more events at large k.
  - The data k_{min} distribution has more events at small k.

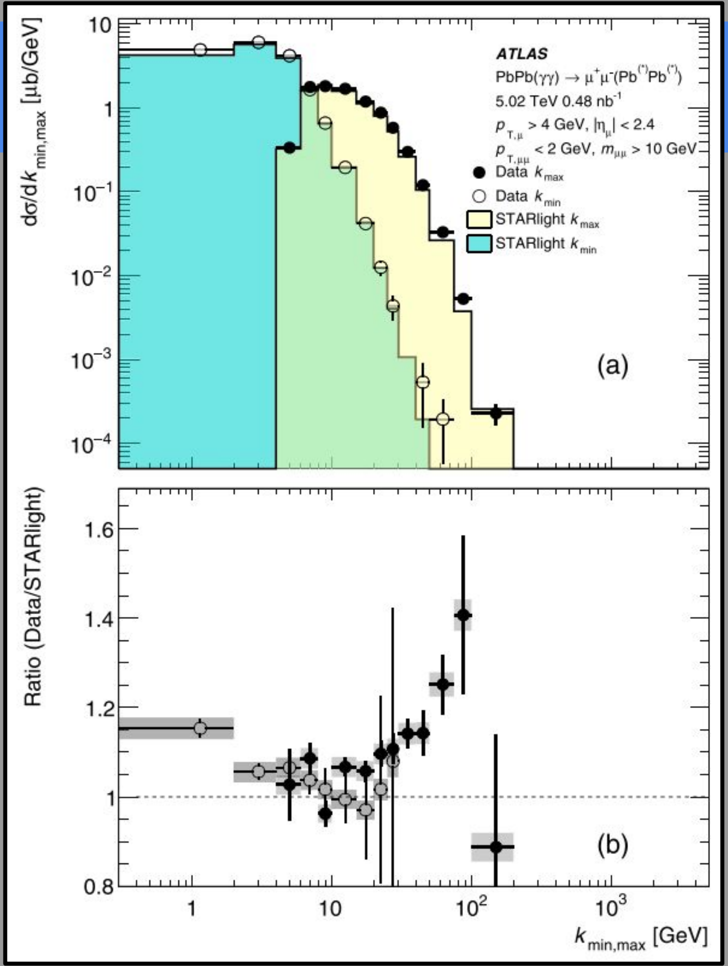

Dimuon Photoproduction… But Not in UPC

- Without enforcing the UPC condition with the ZDC, photoproduction of dimuons still occurs.
  - ATLAS has studied how this process evolves with collision centrality.
  - These results provide an update to a Run 1 measurement, now with enhanced statistics.
- This measurement uses photoproduction as a purely EM probe of the Quark-Gluon Plasma.
  - This interpretation requires a strong understanding of the initial state photon properties.

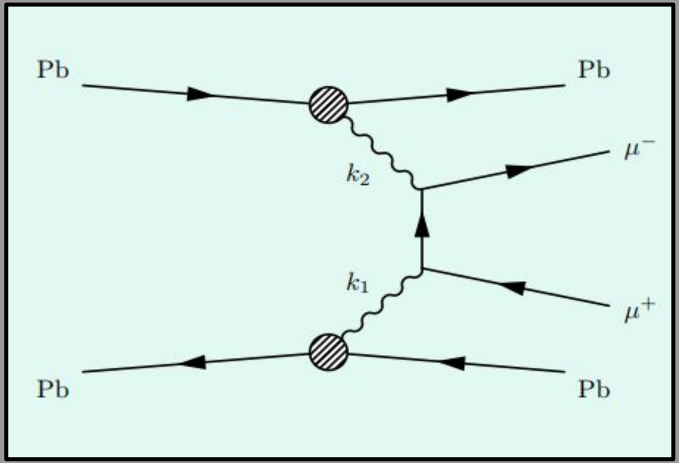

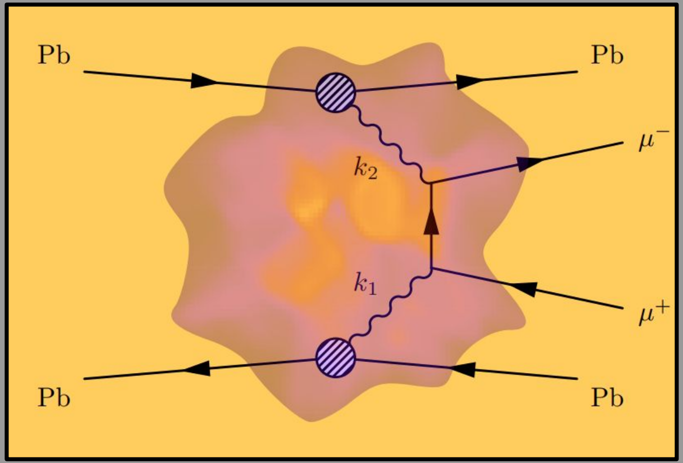

Non-UPC Dimuons: Centrality Dependence

- We transition to $k_\perp$ to describe the deflection (defined below) since it does not exhibit a p_T dependence which is observed in $\alpha = 1 - |\Delta\phi|/\pi$.
- The data $k_\perp$ distribution shows a centrality-dependent peak not seen in the STARlight MC.

$$k_\perp \equiv (p_{T1} + p_{T2})\,|(\pi - \Delta\phi)|/2$$

Central ← UPC

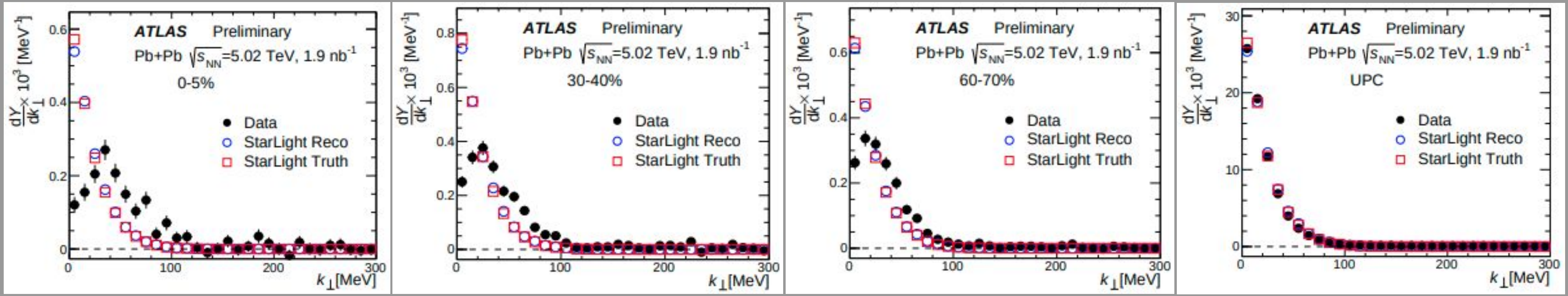

Non-UPC Dimuons: Theory Comparisons

- Several recent theoretical predictions offer explanations for the suppression at small $k_{\perp}$.
  - QED-Based interference effects (Zha, Brandenburg, Tang, Xu): https://arxiv.org/abs/1812.02820
  - Generalized EPA (Klein, Mueller, Xiao, Yuan): https://arxiv.org/abs/2003.02947
  - Photon Wigner Distributions (Klusek-Gawenda, Schäfer, Szczurek): https://arxiv.org/abs/2012.11973
- A comparison to ATLAS data from the third calculation is shown below, with the suppression at 0.

Central ← Peripheral

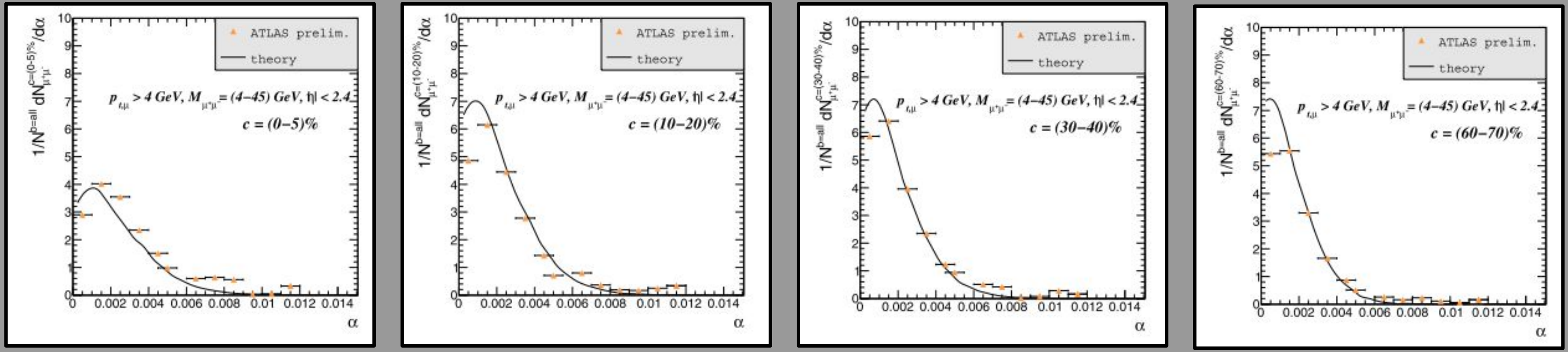

Non-UPC Dimuons: Extracting Shape Information

- The distribution moments are a model-independent demonstration of the variation with centrality.
  - The first moment shows statistically significant variation over the centrality range.
  - The standard deviation does not significantly vary.

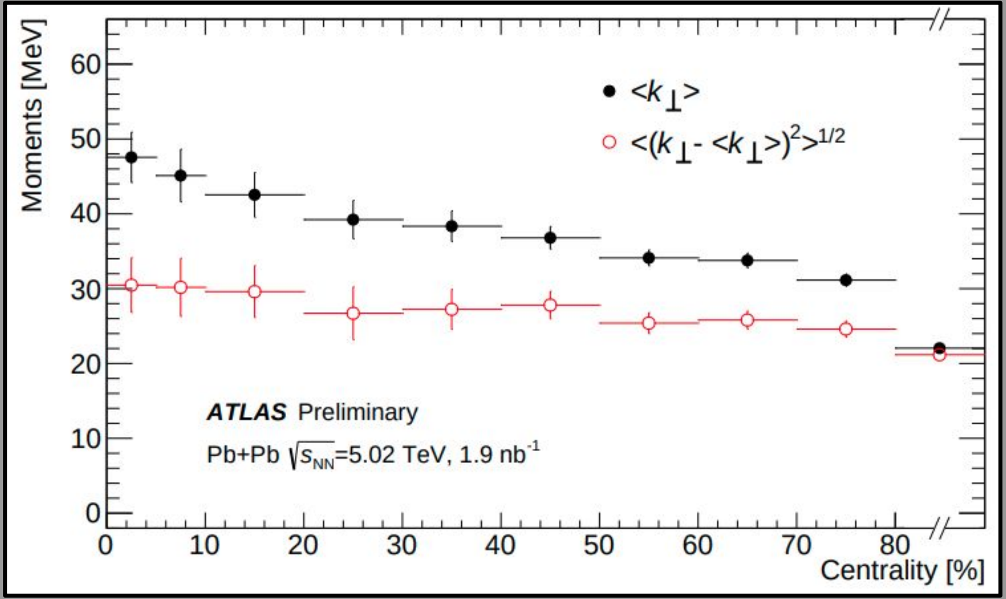

Light-By-Light Scattering in ATLAS

- Light-by-light scattering is a process forbidden in classical electrodynamics, which only occurs due to quantum mechanical effects.
  - The leading-order contribution is the box diagram shown on the left.
- This analysis is sensitive to the existence of Axion-Like Particles (ALPs), a potential BSM particle which would contribute to this cross-section through the diagram on the right.

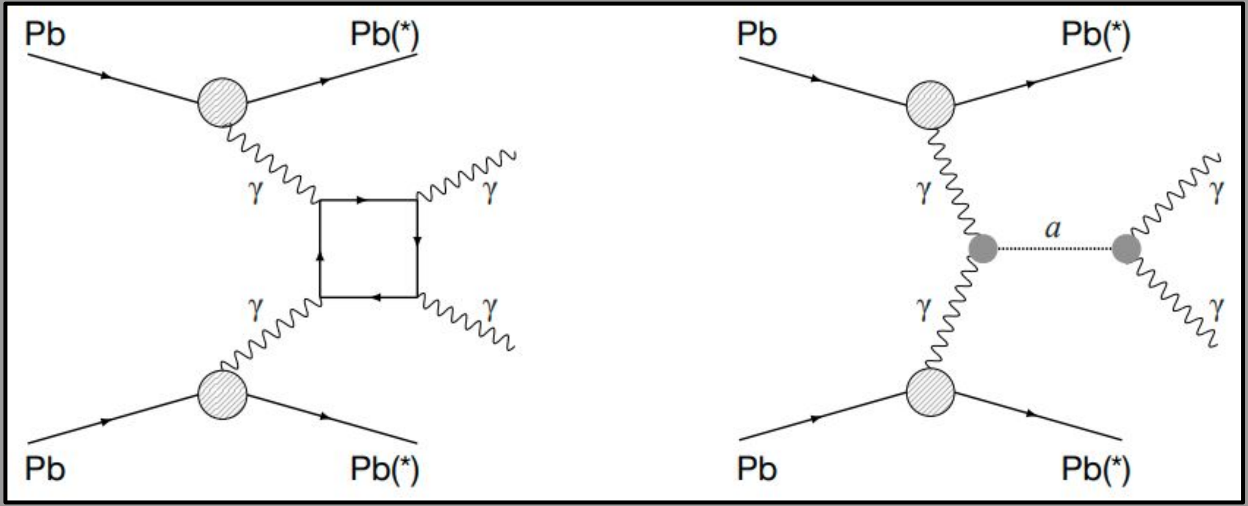

Differential $\gamma\gamma \rightarrow \gamma\gamma$ Cross-Sections

- The fiducial cross-sections for $\gamma\gamma \rightarrow \gamma\gamma$ scattering were measured differentially in several key variables in this measurement.
  - The MC comparison using SuperCHIC highlights regions where excess cross-section is observed.

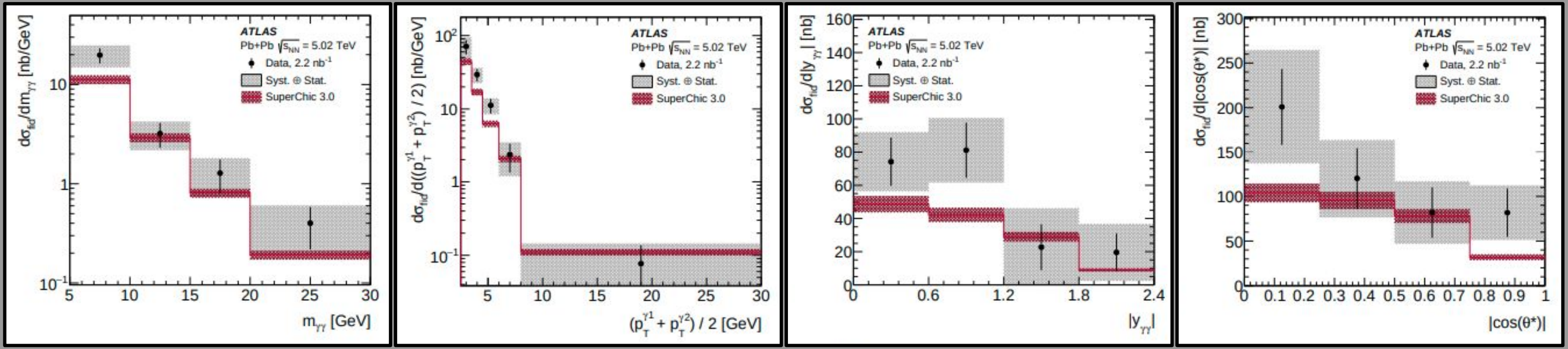

Differential $\gamma\gamma \rightarrow \gamma\gamma$ Cross-Sections

- The fiducial cross-sections for $\gamma\gamma \rightarrow \gamma\gamma$ scattering were measured differentially in several key variables in this measurement.
  - The MC comparison using SuperCHIC highlights regions where excess cross-section is observed.
- The diphoton invariant mass distribution is a key test for setting ALP limits.

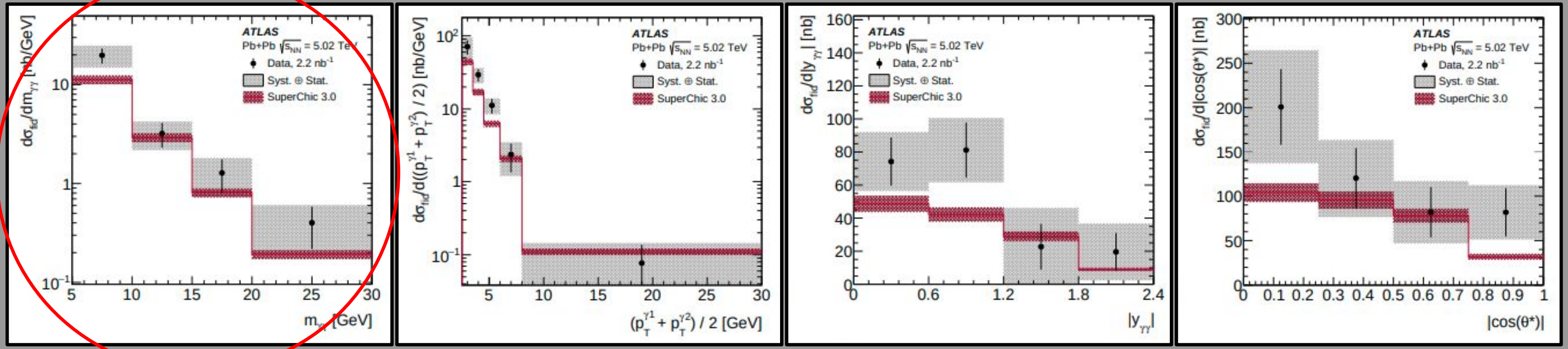

Setting Axion-Like Particle Limits with $m_{\gamma\gamma}$

- After accounting for background contributions, simulations using STARlight which incorporates ALPs with variable mass and coupling.
  - Since no substantial ALP signal is found, these simulations are used to set limits with a 95% confidence interval in mass-coupling space.
- A 100% ALP to diphoton branching ratio is assumed for a conservative limit.

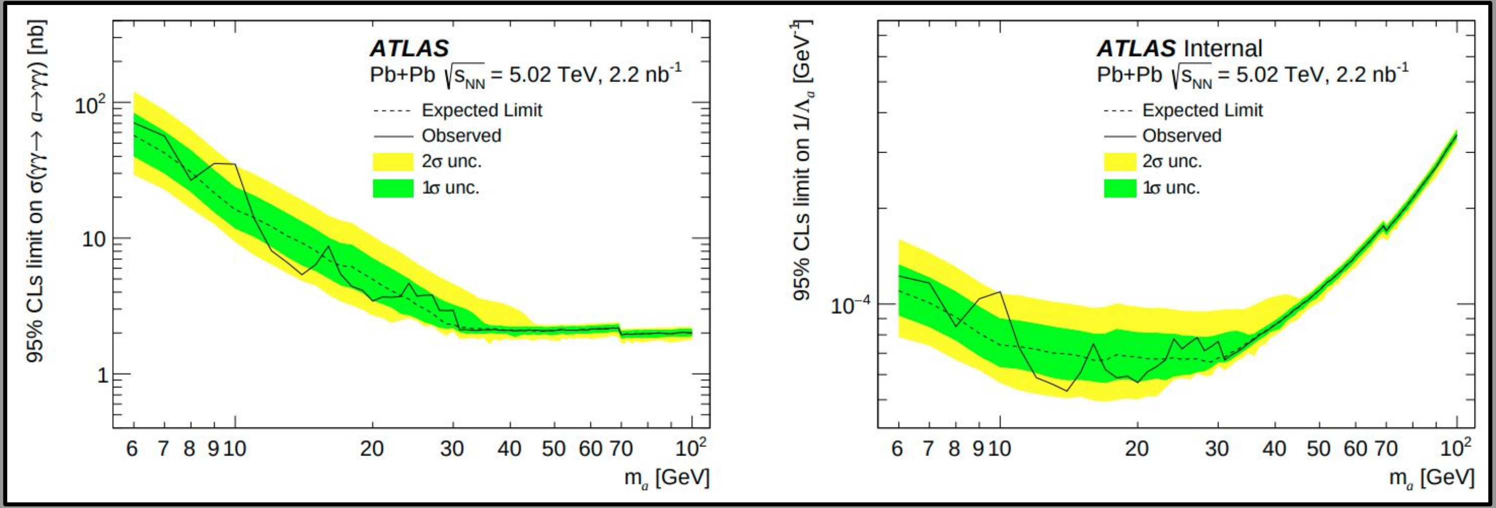

Context of World ALP Limits

- In the context of previous limits set on ALPs, this result extends the 2019 limit set by CMS.
  - The limit roughly covers the same m_a space, but down to lower coupling.

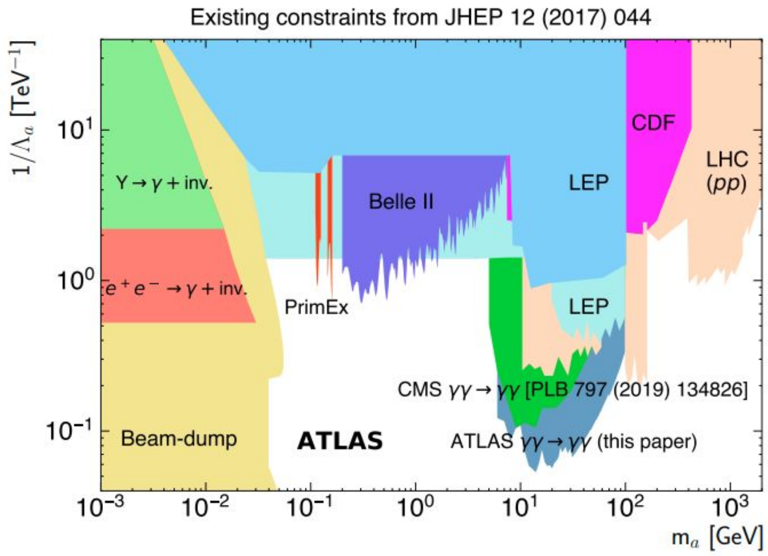

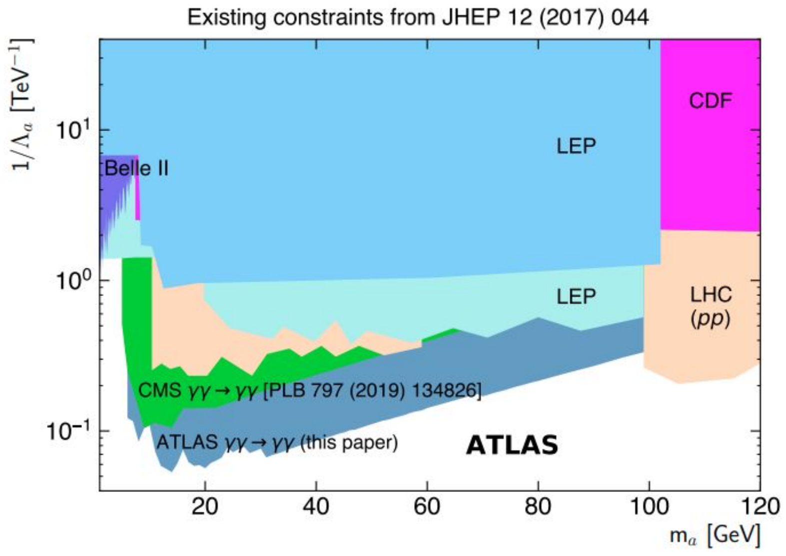

Photonuclear Two-Particle Correlations in ATLAS

- Two-particle correlations arising from the hydrodynamic evolution of QGP are a well-established property of heavy ion collisions.
  - In smaller systems such as *pp* collisions, these correlations are also observed.
  - In UPC, we have access to an even smaller collision system, γA.

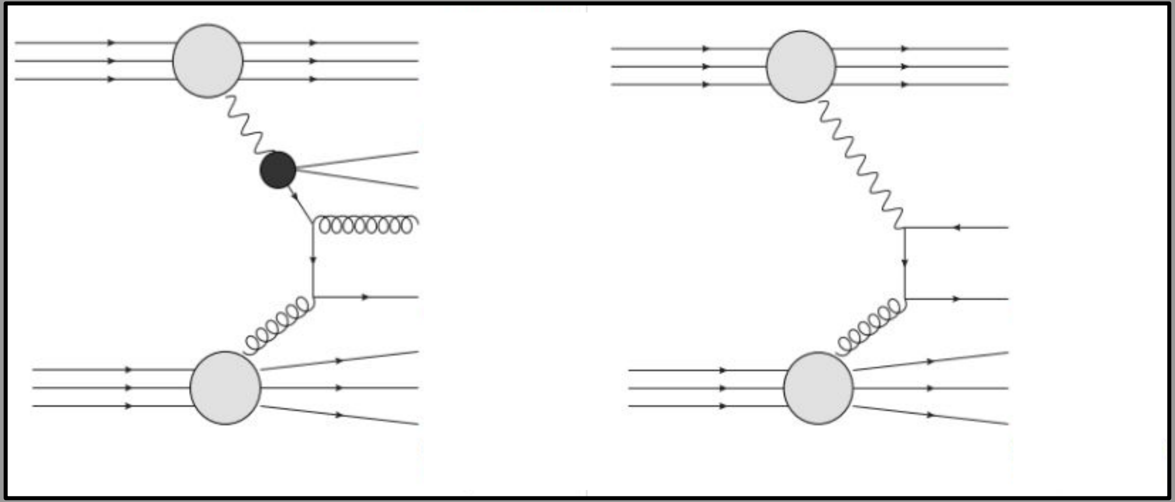

Photonuclear Two-Particle Correlations in ATLAS

- Two-particle correlations arising from the hydrodynamic evolution of QGP are a well-established property of heavy ion collisions.
  - In smaller systems such as *pp* collisions, these correlations are also observed.
  - In UPC, we have access to an even smaller collision system, γA.
- Because of the asymmetric collision system, rapidity gaps are a signature of these events and can be used to select them.

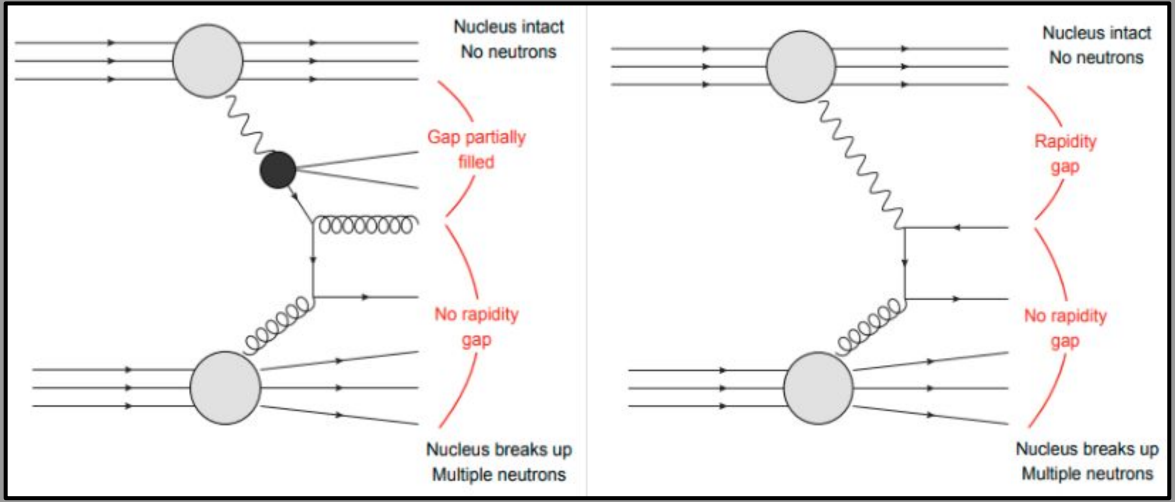

Rapidity Gap Requirements

- The event multiplicity distribution is very different for gap selections, showing 2 different kinds of events passing the 0nXn ZDC requirement.

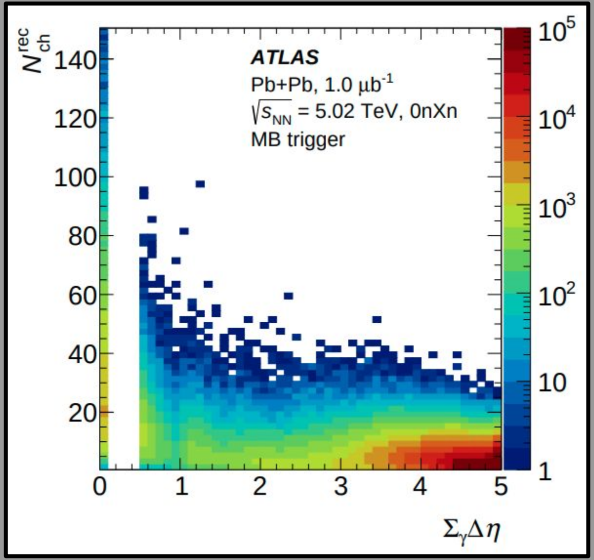

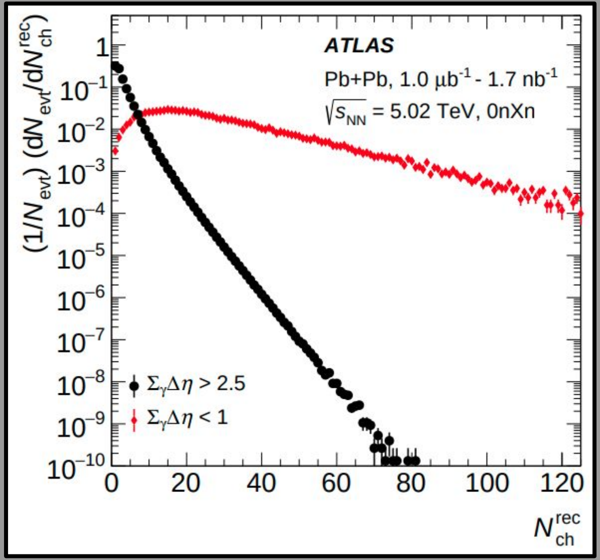

Rapidity Gap Requirements

- The event multiplicity distribution is very different for gap selections, showing 2 different kinds of events passing the 0nXn ZDC requirement.
  - The red points are hadronic events with large multiplicities and small gaps.
  - The black points are photonuclear events with smaller multiplicities and large gaps.

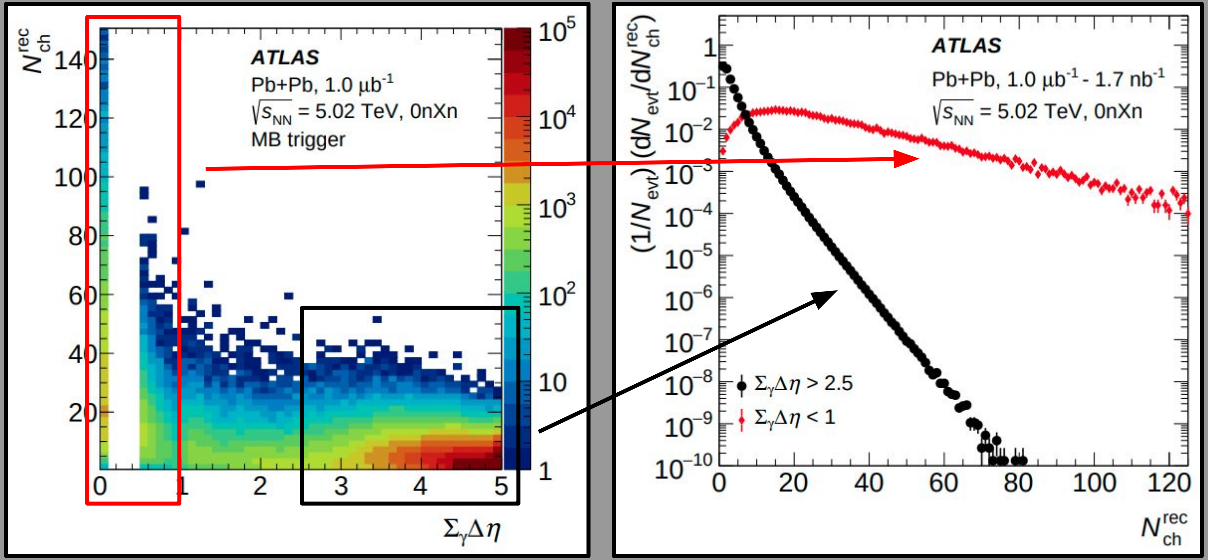

$\Sigma_\gamma\Delta\eta$ is determined by summing all gaps greater than 0.5 on the photon-going side of the event.

Template Fitting the Ridge

- After selecting these events, the correlation functions are constructed in bins of N_{ch} and p_T, as shown on the right.

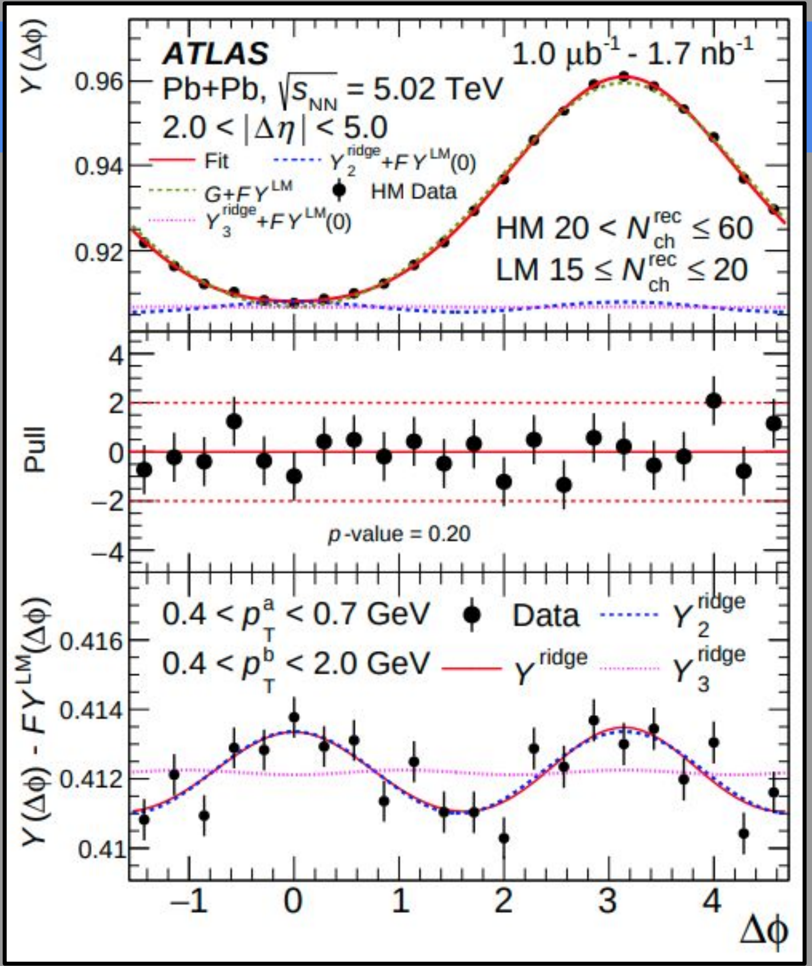

Template Fitting the Ridge

- After selecting these events, the correlation functions are constructed in bins of N_{ch} and p_T, as shown on the right.
- A template fitting procedure is applied and the non-flow contribution is subtracted, yielding the bottom panel.
- After subtraction, the v_n coefficients are extracted by fitting Fourier harmonics, as shown in the fits to the bottom panel.

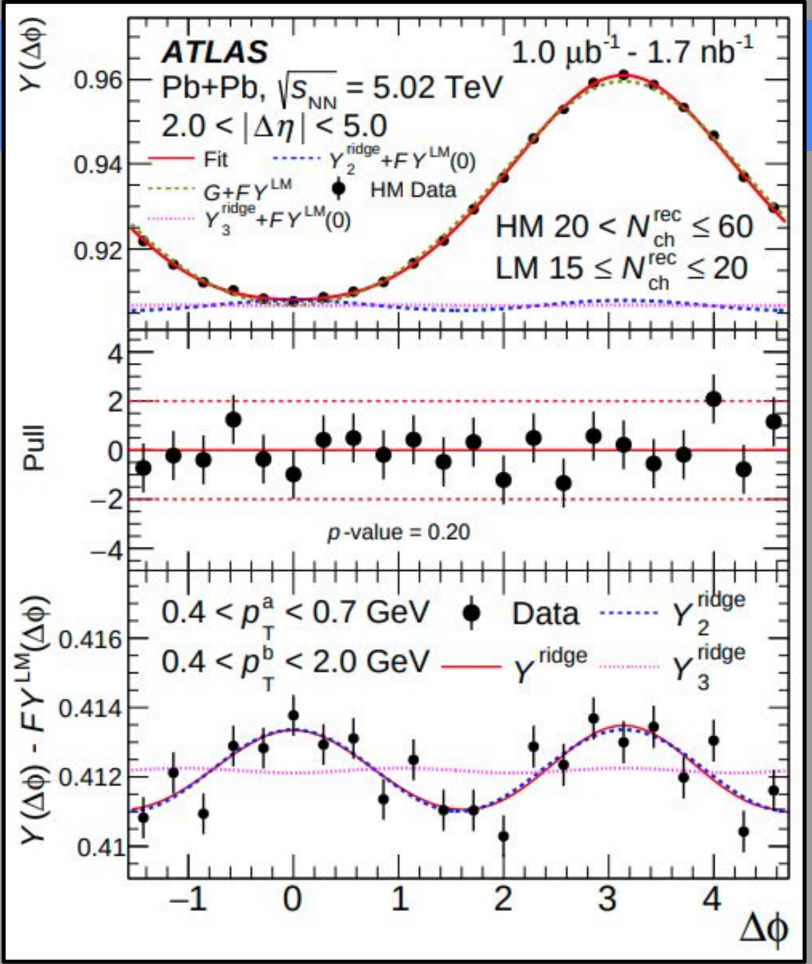

Determining $v_n(N_{ch})$ in Photonuclear Collisions

- The v_2 and v_3 coefficients are shown here as a function of N_{ch}.
- The v_2 is clearly non-zero and does not vary significantly with N_{ch}.
  - The photonuclear v_2 is about ⅔ the value in *pp* and *p*+Pb.
- The v_3 is smaller and also does not vary with N_{ch}.
  - It is consistent with the v_3 seen in *pp* and *p*+Pb due to large uncertainties.

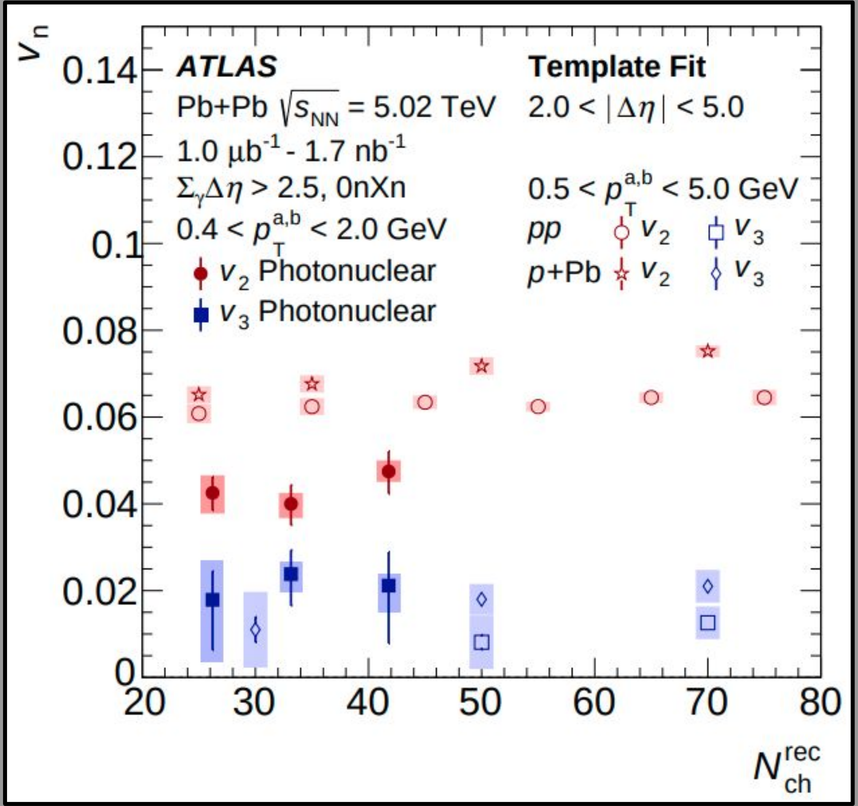

Comparing $v_2(p_T)$ to CGC Predictions

- The low-p_T v_2 is consistent with the CGC calculation of γA v_2 (Shi et al., 2008.03569 [hep-ph]).
  - The theoretical uncertainty arises from hadron fragmentation.

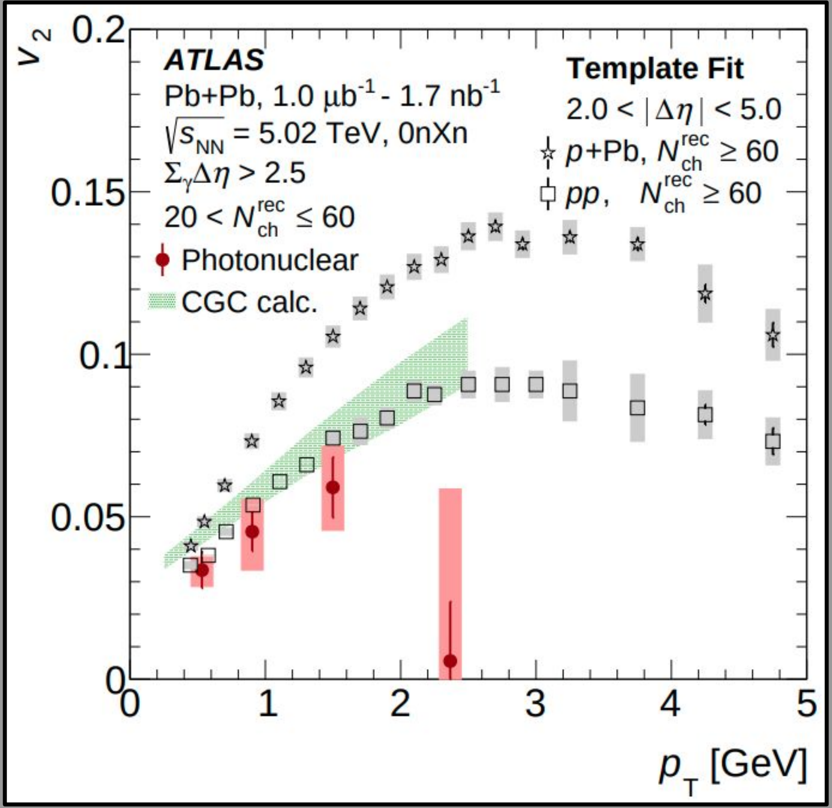

Summary

- Ultra-peripheral collisions provide a useful new tool to study a wide array of physics via a number of different photon-scattering mechanisms.
  - ATLAS has already used UPCs to study everything from BSM physics searches to collectivity in small systems.
  - UPC results such as $\gamma\gamma\rightarrow\mu^+\mu^-$ scattering provides a critical test of the theory.
    - This theory then allows ATLAS to use $\gamma\gamma\rightarrow\mu^+\mu^-$ in hadronic Pb+Pb collisions as an EM probe of Quark-Gluon Plasma.

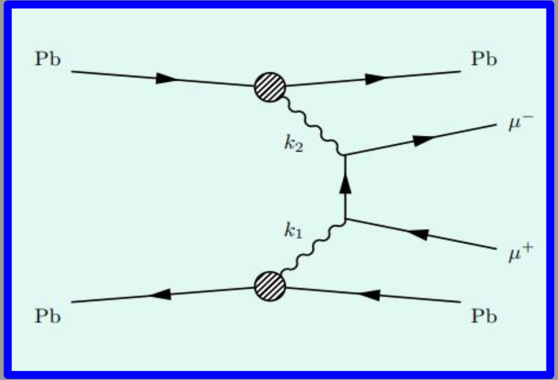

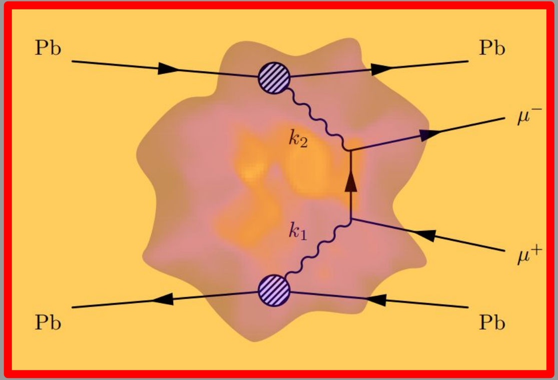

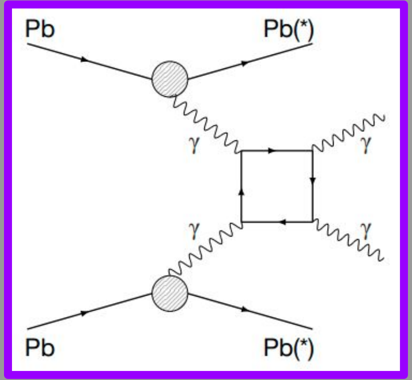

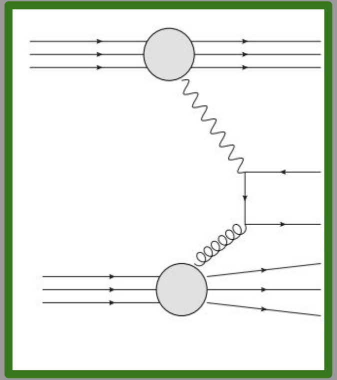

Backup

ZDC Topology in UPC Dimuon Production

- The ZDC measures neutrons in the region $|\eta| > 8.3$, signaling nuclear breakup.
  - The energy in each of the ZDCs form an event “topology” and define several event classes.

1 neutron peak

2 neutron peak

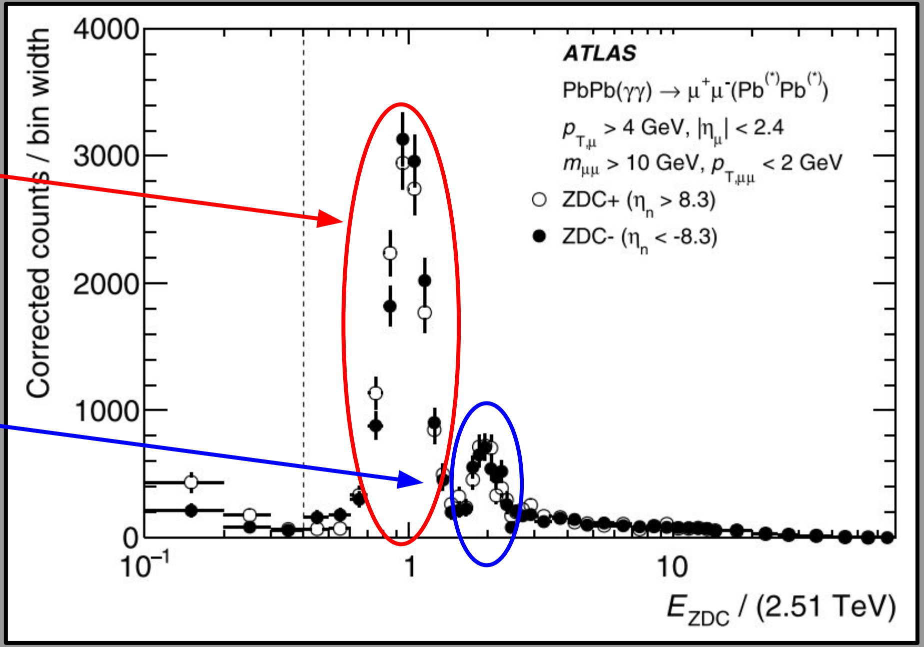

Differential $\gamma\gamma\rightarrow\gamma\gamma$ Kinematics

- The recent light-by-light scattering measurement includes a much more differential look at diphoton kinematics.
  - The MC is scaled to have the same integrated luminosity as the data for this comparison.
  - These distributions confirm consistency with the simulated data + background.

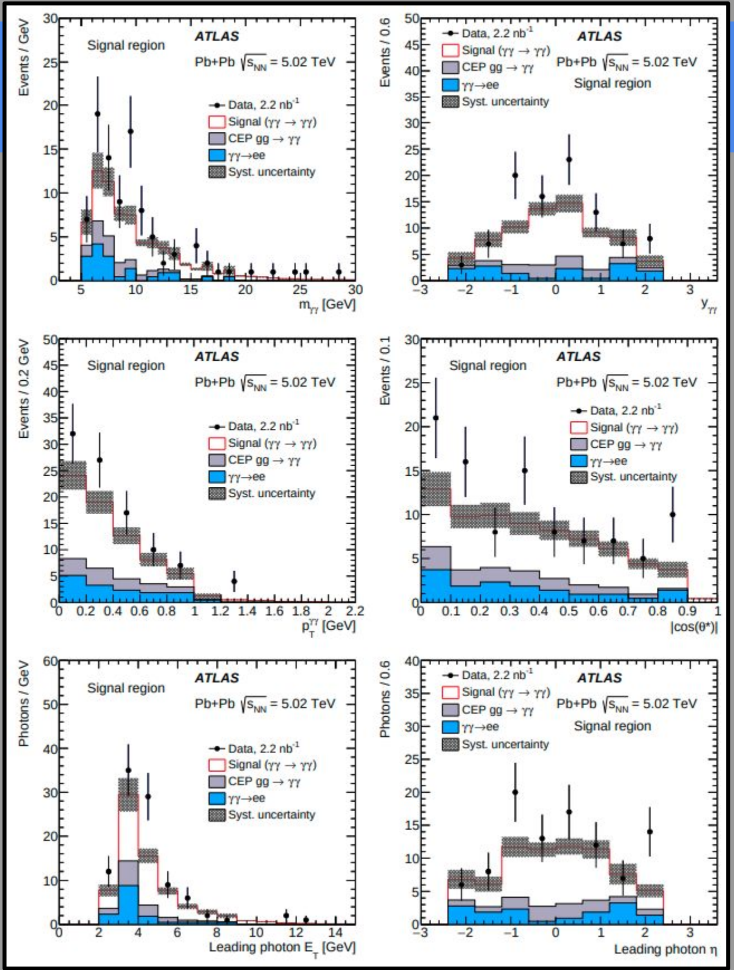

Separating Central Exclusive Photon Production

- A key background to this measurement is Central Exclusive Photon (CEP) production.
  - Instead of $\gamma\gamma \rightarrow \gamma\gamma$, two gluons can interact to produce photons via $gg \rightarrow \gamma\gamma$.
- It is mostly removed by an acoplanarity cut at 0.1 (shown below), and the residual background in the signal region is subtracted.

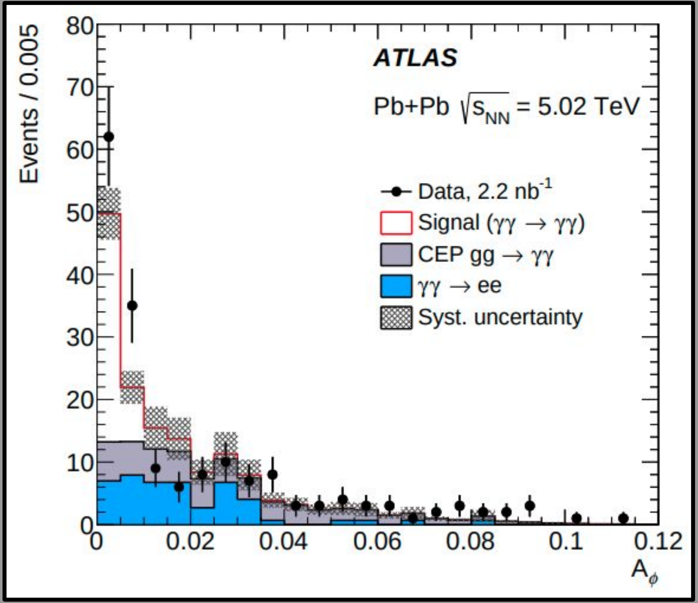

Non-UPC Dimuon Photoproduction: Observables

- The primary background for this analysis is muon pairs produced via decays of heavy flavor quarks, which is subtracted via a template fitting procedure.
- The acoplanarity exhibits a p_T-dependence which can obscure centrality-dependent effects.

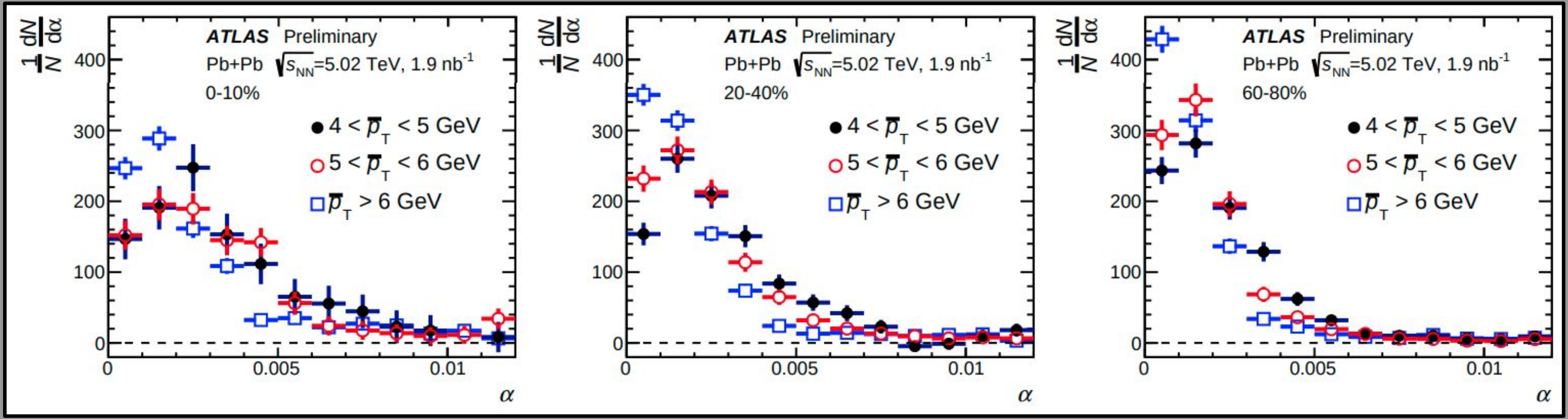

Non-UPC Dimuon Photoproduction: Observables

- The primary background for this analysis is muon pairs produced via decays of heavy flavor quarks, which is subtracted via a template fitting procedure.
- The acoplanarity exhibits a p_T-dependence which can obscure centrality-dependent effects.
- To better describe the angular deflection of the dimuon pair, a new variable is introduced, $k_\perp$.

$$k_\perp \equiv (p_{T1} + p_{T2})\,|(\pi - \Delta\phi)|/2$$

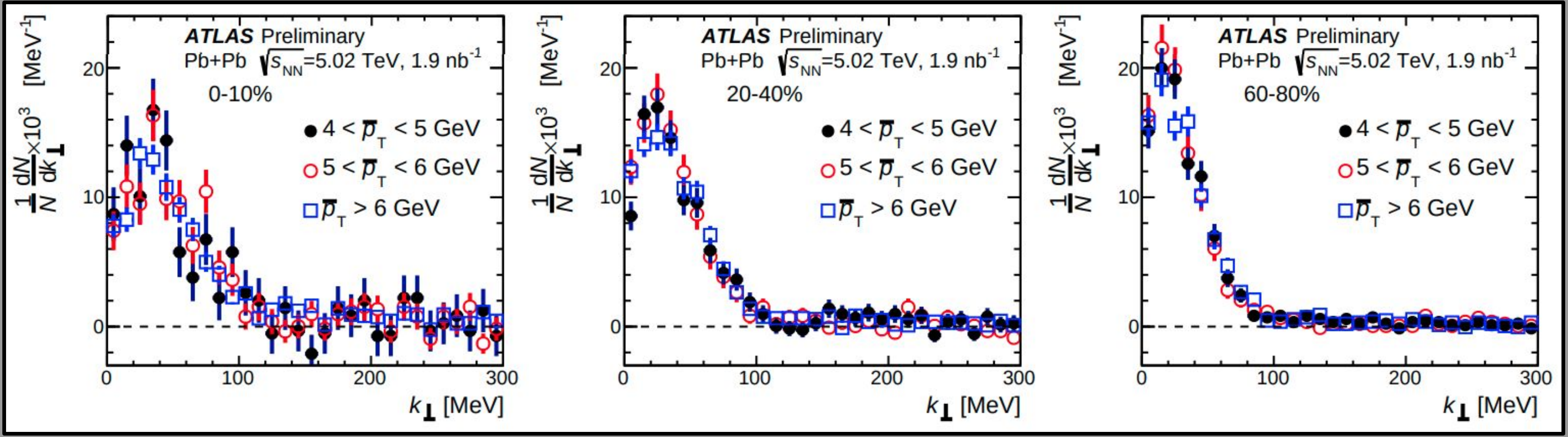

Rapidity Gap Requirements

- The event multiplicity distribution is very different for gap selections, showing 2 different kinds of events passing the 0nXn ZDC requirement.
- In the MC comparison, the transition of data agreeing with Pb+Pb MC to γ+p/Pb MC is clearly visible around 2-2.5.

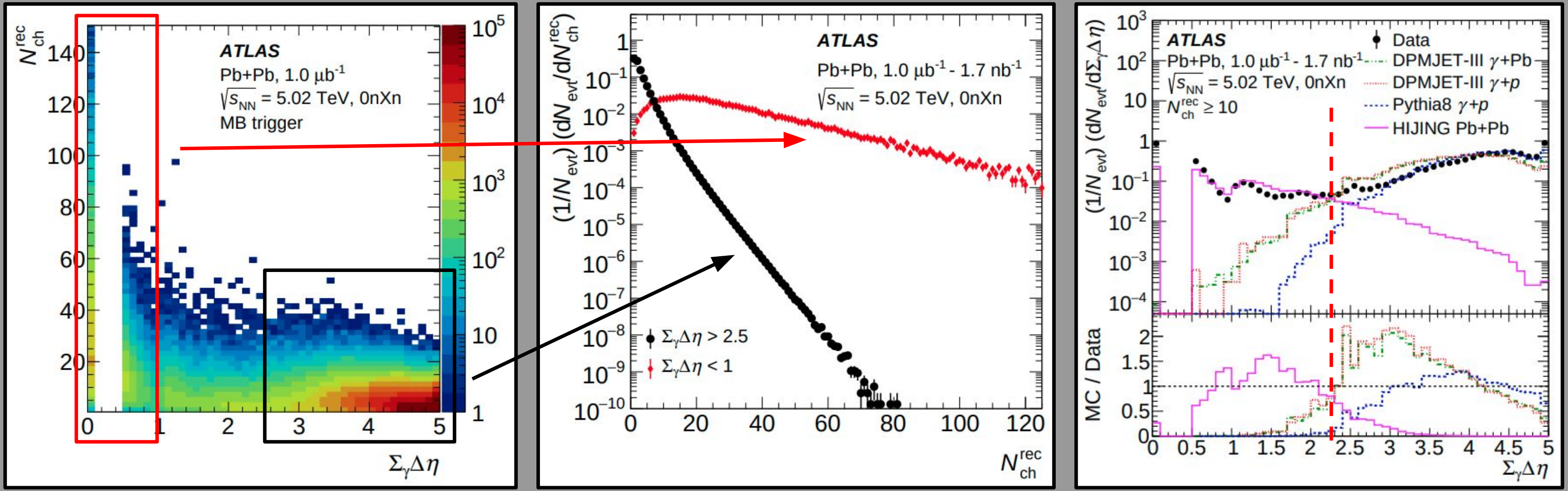

Photonuclear dN/dη

- Above N_{ch} = 5, the dN/dη distribution of photonuclear events is quite consistent.
  - MC captures the different multiplicity regions well but not the dN/dη.
- None of the MC generators quite capture the shape of the dN/dη distribution.